Giant Mutual Proximity Effects in Ferromagnetic/Superconducting Nanostructures

V. T. Petrashov,[1] I. A. Sosnin,[1,2] I. Cox,[1] A. Parsons,[1] and C. Troadec[1]
[1]*Department of Physics, Royal Holloway, University of London, Egham, Surrey TW20 0EX, United Kingdom*
[2]*Institute of Microelectronics Technology, Russian Academy of Sciences, Chernogolovka, Moscow District, 142432 Russia*
(Received 1 December 1998; revised manuscript received 16 March 1999)

A strong mutual influence of superconductors (S) and ferromagnetic (F) conductors in hybrid F/S (Ni/Al) nanostructures is observed. The proximity-induced conductance on the F side, ΔG, is 2 orders of magnitude larger than that predicted by theory. A crossover from positive to negative ΔG takes place upon an increase in the F/S interface barrier resistance. Reentrance of the superconductors to the normal state reciprocated by changes on the F side has been found in low applied magnetic fields with new peaks in the differential resistance as an effect of the saturation magnetization. An analysis has been developed providing a base for a numerical description of the system.

PACS numbers: 74.50.+r, 74.80.Fp, 85.30.St

At the interface of a normal metal (N) to a superconductor (S), normal electrons coherently evolve into holes retracing the electrons on the N side and creating Cooper pairs on the S side and *vice versa*. This process, called the Andreev reflection [1], is a key to the microscopic mechanism of the superconducting proximity effect. In ballistic normal conductors when the bulk scattering is negligible the transport properties are directly connected to the probabilities of the scattering processes at the N/S interfaces [2]. In the general case of conductors with diffusive electron transport, the connection is much more complex resulting in many spectacular unconventional proximity effects (see [3] for a review). Among the highlights of recent investigations is the discovery of the long-range phase-sensitive effects and the reentrance of diffusive proximity conductors to the normal state at low quasiparticle energy [4]. Theory provides several strong arguments that these effects are specific to "nonmagnetic" conductors and are unobservable in disordered ferromagnetic (F) conductors. The arguments are based on several fundamental differences between N/S and F/S systems. While an Andreev reflection conserves energy and components of the momentum parallel to the F/S interface of incident and reflected quasiparticles, they occupy opposite spin bands. In a ferromagnet with different numbers of spin-up, $n_\uparrow$, and spin-down, $n_\downarrow$, conduction channels, only a fraction $n_\downarrow/n_\uparrow$ of the majority $n_\uparrow$ channels can be Andreev reflected [5] making a superconductor an effective spin filter. Furthermore, in a ferromagnet with the exchange field energy, h_0, the Andreev reflected quasiparticles acquire a momentum of $Q = 2h_0/\nu_F$, where ν_F is the Fermi velocity [6]. The latter results in fast oscillating superconductor-induced wave functions exponentially decaying in diffusive conductors over microscopic distances, $\xi_m = \sqrt{(\hbar D/2\pi k_B T_0)}$, where $T_0 \approx h_0/k_B$ is the Curie temperature; D is the diffusion constant. These short-range effects have been intensively studied in the superlattices comprising thin F and S layers (see, e.g., [7], and references therein). The amplitude of long-range effects in diffusive F/S systems with small superconducting gap, $\Delta \ll h_0$, is predicted to be negligibly small [6].

In this Letter we report on the first observation of giant effects of mutual influence of ferromagnetic conductors and superconductors in hybrid F/S nanostructures. The amplitude and the range of the proximity-induced changes in the conductance on the F side of the structures are found to be more than 2 orders in magnitude larger than those predicted by theory. Dramatic changes in the transport properties on the S side of the system with new peaks in the differential resistance have been observed. A phenomenological analysis of the superconductor-induced effects and a model explaining qualitatively the influence of ferromagnetic conductors are presented.

The samples were fabricated using e-beam lithography. The geometry of the structures is shown in Fig. 1 (see left inset). The bar in the inset shows the actual scale. The width of the wires was about 100 nm. The first layer was a 40 nm thick Ni film in contact with golden pads (left side of the structure). The length-to-width ratio for the Ni wire was about 20. The second layer was Al film of the thickness $d = 55$ nm with a small area of the interface to Ni of about 100×100 nm^2. We took particular care to create clean interfaces and control their composition. Before the deposition of the second layer, the contact area was Ar^+ plasma etched. A study of wide checking layers using the secondary ion mass spectroscopy with Cs^+ ions showed very steep concentration profiles close to a theoretical value for an abrupt interface.

The measurements were carried out using both dc and low frequency lock-in techniques in the temperature range from 0.28 to 1.5 K in magnetic fields up to 5 T applied perpendicular to the substrate. The combination of U_1, I_1 of potential and current electrodes was used to measure the region ab, of the total length $L_{ab} = L_1 + L_2$ which included the region of the length $L = \xi + L_2$, which we call F/S junction; ξ is the distance at which the superconductor is influential in the bulk of the F wire. The use of I_2 or I_3 combined with U_2 enabled measurements of

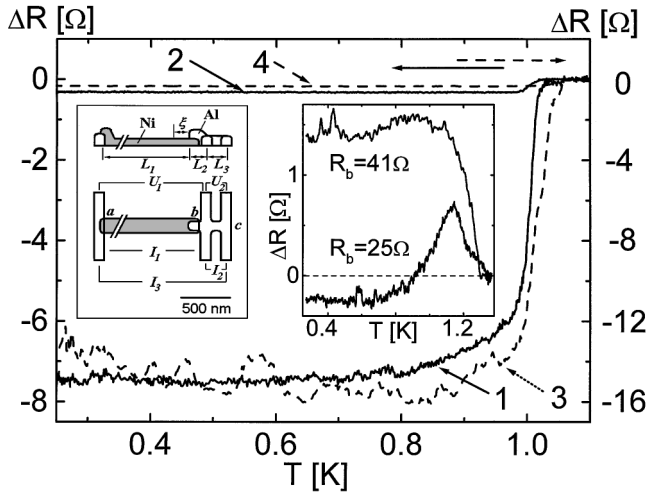

FIG. 1. Temperature dependence of the resistance for F/S junctions (curves 1 and 3) and adjacent superconducting wires (curves 2 and 4) taken at zero external magnetic field, the lines 1 and 2 for the sample FS1 (left axis); lines 3 and 4 for FS3 (right axis) at low F/S interface barrier resistance, R_b. Left inset: sample geometry, side and top views; the bar shows actual scale. Right inset: temperature dependence at high R_b.

the adjacent Al wire of the length L_3, which we call S wire. The resistivity, ρ, and barrier resistance, R_b, was measured directly using on-chip-checking layers. The value of ρ for the Ni and Al films was about 50 and 1.5 $\mu\Omega$ cm, with corresponding diffusion constants, D, of about 10 and 100 cm^2/s, calculated using a ρl value for Ni, 1.5×10^{-11} $\Omega\,\mathrm{cm}^2$ [8(a)] and Al, $3.2 \times 10^{-12}\Omega\,\mathrm{cm}^2$ [8(b)]. The values of the coherence length, ξ, and penetration depth, λ, for our disordered Al films were 180 nm and 140 nm, correspondingly.

Figure 1 shows the temperature dependence of the resistance of F/S junctions and that of the S wires for two samples. The length-to-width ratio for the S wires is equal to that for the Al film overlapping Ni in the junction area. We observe a spectacular drop in the resistance of the F/S junction, ΔR, at the onset of superconductivity with slow changes persisting down to the lowest temperatures. The amplitude of the drop is up to 50 times greater than the resistance of the L_2 region of the junction. Such a *giant change in the resistance together with its sign* can be explained only as due to the *drop in the resistance in the bulk of the F wire* beyond L_2. Moreover, the change in the resistance can be explained only if one assumes that it occurs in the part of the Ni wire of length, ξ (see inset in Fig. 1), much longer than ξ_m. For our Ni wires we find $\xi_m \approx 2$ nm with $T_0(\mathrm{Ni}) = 630$ K. The contribution of such a small portion of film to the resistance, $\Delta R(\xi_m) = \rho_{\mathrm{Ni}}(\xi_m/A)$, is 2 orders of magnitude smaller than the measured drop; A is the cross-section area. We observe a crossover from negative to positive ΔR upon an increase in the barrier contribution (right inset in Fig. 1). To control the value of barrier resistance, R_b, we used its dependence on the ion etching time. The crossover takes place at the barrier resistance $R^*_{\mathrm{Ni/Al}} \approx 27\ \Omega$ corresponding to the specific crossover resistance $AR^*_{\mathrm{Ni/Al}} \approx 2.7 \times 10^{-9}\ \Omega\,\mathrm{cm}^2$. The magnitude of the negative ΔR correlates with the resistivity, ρ_{Ni}, of Ni wires, with no correlation with ρ_{Al}: sample FS1 [$\Delta R = 8\ \Omega$, $\delta = \Delta R/\Delta R(\xi_m) = 0.014$, $\rho_{\mathrm{Ni}} = 52\ \mu\Omega$ cm, $\rho_{\mathrm{Al}} = 1.0\ \mu\Omega$ cm]; FS2 ($\Delta R = 4\ \Omega$, $\delta = 0.038$, $\rho_{\mathrm{Ni}} = 44\ \mu\Omega$ cm, $\rho_{\mathrm{Al}} = 1.3\ \mu\Omega$ cm); FS3 ($\Delta R = 18\ \Omega$, $\delta = 0.01$, $\rho_{\mathrm{Ni}} = 90\ \mu\Omega$ cm, $\rho_{\mathrm{Al}} = 1.5\ \mu\Omega$ cm); FS4 ($\Delta R = 3\ \Omega$, $\delta = 0.03$, $\rho_{\mathrm{Ni}} = 40\ \mu\Omega$ cm, $\rho_{\mathrm{Al}} = 1.5\ \mu\Omega$ cm).

Dramatic changes in the transport properties on the F side and those on the S side are illustrated in Fig. 2. The diagrams show the dependence of differential resistance, dV/dI, on the applied dc current, at different magnetic fields. The curves are taken with the same current leads, I_3 for both, F/S junction and S wire. Several unusual features are seen in the resistance of the S wire. The peaks corresponding to the onset of superconductivity split with the separation of new peaks increasing with lowering magnetic fields [Fig. 2(b)]. The lower current peak position approaches zero [see also Fig. 2(d)] showing that the superconductor *reenters the normal state*. The large amplitude of changes induced in F wires strongly correlates with those on the S side of the structure [Figs. 2(a), 2(b), and 2(c)]. The samples showed usual negative magnetoresistance [9] with $\Delta R \approx 0.1\ \Omega$ at temperatures above the superconducting transition.

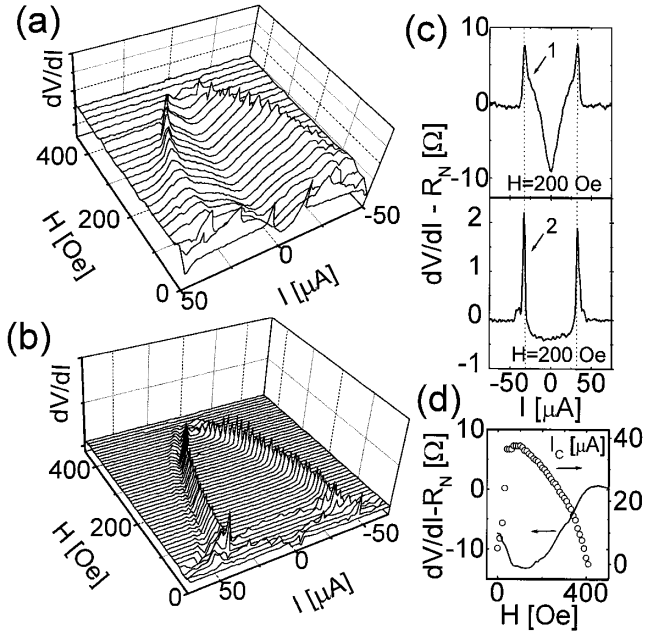

FIG. 2. Differential resistance at different applied dc current and magnetic field (a) for F/S junction, (b) S wire (Al L_3 wire; see inset in Fig. 1). (c),(d) Sections at $H = 200$ Oe for F/S junction (curve 1) and S wire (curve 2). (d) Solid line: magnetic field dependence of the differential resistance of F/S junction at zero bias, left axis; open circles: critical current of the S wire [lower current peaks of Fig. 2(b)], right axis.

To carry out a numerical analysis of the experimental data we will use a phenomenological approach. The conductance of a diffusive F wire can be written as $G_{FN} = (e^2/h)N$, where N is the number of electron levels in the bandwidth of Thouless energy, $\varepsilon_{\rm Th}$ (see [10], and references therein). When spin channels do not mix, the formula can be written in terms of numbers of spin-up (majority spins), $n_\uparrow$, and spin-down, $n_\downarrow$, conduction channels in the Thouless bandwidth: $G_{FN} = (e^2/h)(n_\downarrow + n_\uparrow) \equiv (2e^2/h)n_\downarrow + (e^2/h)(n_\uparrow - n_\downarrow)$. The term proportional to the difference of $(n_\uparrow - n_\downarrow)$ describes spin-polarized current. A formula for the proximity modified conductance, G_{FS}, can be written as $G_{FS} = \eta(2e^2/h)n_\downarrow + \eta_p(e^2/h)(n_\uparrow - n_\downarrow)$ with phenomenological parameters, η and η_p ($0 \le \eta_p \le 1$) matching the current in the F wire with spinless current in the superconductor. The values of η and η_p are connected with the measured changes in the resistance, $\Delta R_{FS} = R_{FN} - R_{FS}$, by

$$\frac{\Delta R_{FS}}{R_{FN}} = 1 - \frac{1}{\eta[1 - P(1 - \alpha)]}, \qquad (1)$$

where $P = |n_\uparrow - n_\downarrow/n_\uparrow + n_\downarrow|$ is the spin polarization, $\alpha = \eta_p/\eta$, $R_{FN} = \rho_F \xi_{\rm kin}/w d_F$, $\varepsilon_{\rm Th} = \hbar D/\xi^2_{\rm kin}$, $\xi_{\rm kin} = \min(L_\varphi, L)$, L_φ is the phase breaking length including spin-relaxation processes, and L is the length of the wire. The limit of $\alpha \to 0$ corresponds to the total spin filtering.

The formula (1) coincides with that suggested in [5] for a ballistic contact ($\eta = 2$) in the limit of $\alpha \to 0$, however there is a principal difference: for a ballistic junction, $n_\uparrow$ and $n_\downarrow$ are the numbers of spin-up and spin-down transverse modes in the contact at the Fermi level [5].

In the limit of $P \to 0$ the formula (1) has the structure similar to that established for nonmagnetic normal disordered metals [3]. In general, the value of η is varying in the range $1 < \eta < 2$. A microscopic mechanism of the enhancement of conductance by the factor of η in nonmagnetic metals is based on the Andreev reflection. Here we consider η as a phenomenological parameter.

Several important conclusions can be drawn when the polarization is known. Substituting into (1) the measured values for ΔR_{FS}, the resistivity and the *upper bound* for the right-hand side of the equation we estimate the *lower bound* for the coherence length. With $P = 0.23$ for Ni reported in [11], we get values of $\xi_{\rm kin}$ in the range of 0.2 to 0.6 μm for our samples, with $\xi_{\rm kin}/\xi_m > 10^2$ for all samples investigated. If finite spin-polarized current is allowed in the F-junction area the value of $\xi_{\rm kin}$, accounting for the measured values of ΔR_{FS}, is even larger by a factor of about $(1 + P) \approx 1.25$.

To account for experimentally observed positive values of $\Delta R_{FS} = R_{FN} - R_{FS} > 0$, the value of η must be large enough: $\eta > \eta_0 = 1/(1 - P) = 1.3$ in our Ni wires. In general, as it follows from our analysis, the sign of the change in the resistance of ferromagnetic conductors (1) may be positive as well as negative, depending on the values of the parameters $1 \le \eta \le 2$, $0 \le P \le 1$, and $0 \le \alpha < 1$. If the values of the parameters change due to the dependence on the energy of quasiparticles and/or current induced effects, as a result of the competition of the spin filtering and conductance enhancement a crossover from the negative values of ΔR_{FS} to the positive ones may take place as a function of the bias voltage and/or temperature in the vicinity of $\eta[1 - P(1 - \alpha)] \approx 1$ with extrema at certain temperature and bias voltage. These effects have probably been observed in the experiments with Co/Al structures reported recently [12]. The results shown in the inset of Fig. 1 can be interpreted as due to suppression of η at high barrier resistance.

The phase diagram shown in Fig. 2(a) can be explained as due to the influence of the magnetization of the F electrode on the S wire. The dependence of the critical current on a magnetic field, H, can be written as $J_c(H) = J_0(\Delta(H)/\Delta_0)^{3/2}$, J_0 and Δ_0 are the values of critical current and the gap at zero magnetic field and temperature [13]. The magnetic field, $\mathbf{H}^*$, that the S wire is subjected to, depends strongly on the angle, between the substrate and the saturation magnetization, $\mathbf{M}_s$. The latter rotates from the parallel to the substrate direction, to that parallel to the easy axis, upon the application of a relatively low field, $H = H_{\rm rot}$, perpendicular to the substrate. As a result the modulus of $\mathbf{H}^*$ varies from the rather high value of $|\mathbf{B}_s| \approx 4\pi|\mathbf{M}_s| \approx 6 \times 10^3$ G to the relatively low values at $H > H_{\rm rot}$. Taking into account the boundary conditions, we take the perpendicular to the substrate component of $\mathbf{H}^*$, $H_\perp = H^* \cos(\theta)$, equal to the external field, H, and parallel one, $H_\parallel = H^* \sin(\theta)$, equal to the parallel to the substrate component of $\mathbf{B}_s$. For the dependence of the angle, θ, between the normal to the substrate and $\mathbf{H}^*$ we use the following rotation model: $[H_\parallel/B_s - \sin(\theta_0)]^2 + (H/H_{\rm rot})^2 = 1$, θ_0 is the angle between the easy axis and the normal. The value of the critical field, H_c, at a given angle θ [13]

$$\left| \frac{H_c(\theta)\cos(\theta)}{H_{c\perp}} \right| + \left(\frac{H_c(\theta)\sin(\theta)}{H_{c\parallel}} \right)^2 = 1. \qquad (2)$$

In our phenomenology we assume that the new peaks are due to the Zeeman splitting and can be connected to the singularities in the density of states of quasiparticles that take place at the following energies [11,14]:

$$\Delta(H) = \Delta_0 \left[1 - \left(\frac{H^*(H)}{H_c} \right)^2 \right]^{1/2} \pm \mu_B H^*(H). \qquad (3)$$

The result of the calculations is shown in Fig. 3(b). Our model nicely explains the features of the phase diagram, supporting the Zeeman mechanism. We used the set of directly measured parameters: $H_{c\perp} = 430$ Oe, $T_c = 1$ K with the value of $H_{\rm rot} = 70$ Oe, close to the coercive force and the value of $H_{c\parallel}$ and θ_0 as fitting parameters.

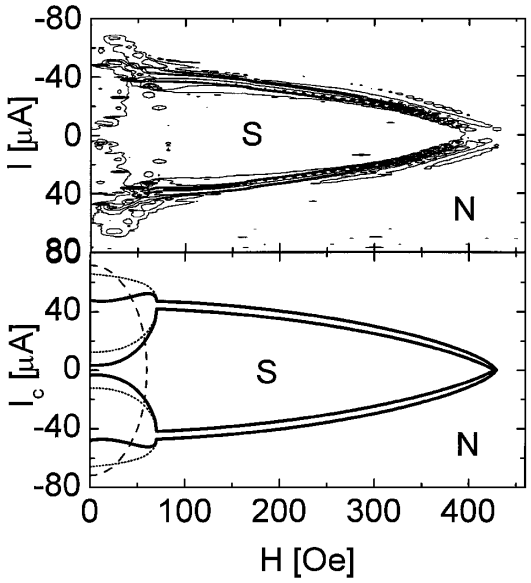

FIG. 3. Normal/superconducting phase diagrams versus current and magnetic field for the S wire (Al L_3 wire; see inset of Fig. 1). (a) Experiment: $dV/dI = \text{const}$ contours of Fig. 2(b). (b) Calculated contours for critical current using formulas (2) and (3); see text. Solid line: $H_{c\parallel} = 8$ kOe, sample FS1, $w = 300$ nm; dotted line: $H_{c\parallel} = 12$ kOe, sample FS2, $w = 100$ nm. Dashed line: the dependence of critical current for Al L_2 wire.

The best fit was obtained with $\theta_0 = 0.1$ and $H_{c\parallel} = 8$ kOe for the sample FS1 with the width $w = 300$ nm of the S wire and $H_{c\parallel} = 12$ kOe for the sample FS2 with $w = 100$ nm. The field $H_\parallel$ induced by the ferromagnetic electrode, unlike the external field, is concentrated in a small volume with the total flux of several flux quanta that may lead to high values of $H_{c\parallel}$. The S wire with lower values of $H_{c\parallel}$ reentered the normal state at low magnetic fields [$j_c(H \to 0) \to 0$]. This accounts for the increase in the resistance of the F/S junction at low fields shown in Fig. 2(d). No low field peaks were observed in the magnetoresistance of narrow samples with higher values of $H_{c\parallel}$, as expected.

The results of Figs. 2 and 3 show that the changes in the resistance of our F wires are mainly due to the influence of the L_3 part of the Al wire rather than overlapping the Al L_2 wire. The dependence of the critical current for the latter is shown in Fig. 3(b) by the dashed line. Interestingly, a minute influence of the L_2 wire is possibly seen in the differential resistance of the L_3 wire; see experimental curves in Figs. 3(a) and 2(b). When the overlap, L_2, is large enough a contribution of the effect of short circuit at the onset of superconductivity becomes important leading to a sharp dip in the resistance at a very low magnetic field $H \approx H_{c\perp}(H_{\text{rot}}/B_s)$ of several Oe, accounting for the results reported in [15].

In summary, we observe a strong mutual influence of ferromagnetic conductors and superconductors in hybrid F/S nanostructures. The saturation magnetization of the ferromagnetic conductors may lead to dramatic changes in the transport properties on the S side of the system resulting in new peaks in the differential resistance and reentrance of the superconductors to the normal state in low external magnetic fields. We suggest a model explaining the effects as due to the Zeeman splitting in the spectrum of quasiparticles. The amplitude and the range of the proximity-induced changes on the F side of the structures are found 2 orders in magnitude larger than those predicted by theory. We observe a crossover from positive to negative proximity-induced conductance upon an increase in the F/S interface resistance. A phenomenological analysis has been developed providing a base for the numerical description of the system. Based on the analysis we anticipate strong effects in hybrid nanostructures comprising superconductors and strongly polarized ferromagnetic materials such as "half-metals." Phase-periodic effects which may exist in F/S nanostructures with long coherence lengths are of great interest.

We acknowledge A. F. Volkov and C. Lambert for valuable discussions. Financial support from the EPSRC (Grant No. GR/L94611) is acknowledged.

[1] A. F. Andreev, Sov. Phys. JETP **19**, 1228 (1964).
[2] S. K. Upadhyay, A. Palanisami, R. N. Louie, and R. A. Burman, Phys. Rev. Lett. **81**, 3247 (1998).
[3] (a) C. J. Lambert and R. Raimondi, J. Phys. Condens. Matter **10**, 901 (1998); (b) C. W. J. Beenakker, Rev. Mod. Phys. **69**, 731 (1997).
[4] (a) V. T. Petrashov, V. N. Antonov, P. Delsing, and T. Claeson, Phys. Rev. Lett. **74**, 5268 (1995); (b) S. Gueron, H. Pothier, N. O. Birge, D. Esteve, and M. H. Devoret, Phys. Rev. Lett. **77**, 3025 (1996); (c) H. Courtois, Ph. Gandit, D. Mailly, and B. Pannetier, Phys. Rev. Lett. **77**, 4950 (1996).
[5] M. J. M. de Jong and C. W. J. Beenakker, Phys. Rev. Lett. **74**, 1657 (1995).
[6] E. A. Demler, G. B. Arnold, and M. R. Beasley, Phys. Rev. B **55**, 15 174 (1997).
[7] J. S. Jiang, D. Davidovic, D. H. Reich, and C. L. Chien, Phys. Rev. Lett. **74**, 314 (1995).
[8] (a) C. Fierz, S.-F. Lee, J. Bass, W. P. Pratt, Jr., and P. A. Schroeder, J. Phys. Condens. Matter **2**, 9701 (1990); (b) P. Santanam and D. E. Prober, Phys. Rev. B **29**, 3733 (1984).
[9] V. T. Petrashov, V. N. Antonov, S. Maksimov, and R. Shaikhaidarov, JETP Lett. **59**, 551 (1994).
[10] S. Washburn and R. A. Webb, Rep. Prog. Phys. **55**, 1311 (1992).
[11] R. Meservey and P. M. Tedrow, Phys. Rep. **238**, 173 (1994).
[12] M. Giroud, H. Courtois, K. Hasselbach, D. Mailly, and B. Pannetier, Phys. Rev. B **58**, 11 872 (1998).
[13] M. Tinkham, *Introduction to Superconductivity* (McGraw-Hill, New York, 1995), 2nd ed.
[14] D. H. Douglass, Phys. Rev. Lett. **7**, 14 (1961).
[15] M. D. Lawrence and N. Giordano, J. Phys. Condens. Matter **8**, L563 (1996).